



University of Dundee

Characterization of Flexor Digitorum Superficialis Muscle Stiffness Using Ultrasound Shear Wave Elastography and MyotonPRO

Tantipoon, Phongpan; Praditpod, Nuttaporn; Pakleppa, Markus; Li, Chunhui; Huang, Zhihong

Published in:
Applied Sciences (Switzerland)

DOI:
[10.3390/app13116384](https://doi.org/10.3390/app13116384)

Publication date:
2023

Licence:
CC BY

Document Version
Publisher's PDF, also known as Version of record

[Link to publication in Discovery Research Portal](#)

Citation for published version (APA):

Tantipoon, P., Praditpod, N., Pakleppa, M., Li, C., & Huang, Z. (2023). Characterization of Flexor Digitorum Superficialis Muscle Stiffness Using Ultrasound Shear Wave Elastography and MyotonPRO: A Cross-Sectional Study Investigating the Correlation between Different Approaches. *Applied Sciences (Switzerland)*, 13(11), [6384]. <https://doi.org/10.3390/app13116384>

General rights

Copyright and moral rights for the publications made accessible in Discovery Research Portal are retained by the authors and/or other copyright owners and it is a condition of accessing publications that users recognise and abide by the legal requirements associated with these rights.

- Users may download and print one copy of any publication from Discovery Research Portal for the purpose of private study or research.
- You may not further distribute the material or use it for any profit-making activity or commercial gain.
- You may freely distribute the URL identifying the publication in the public portal.

Take down policy

If you believe that this document breaches copyright please contact us providing details, and we will remove access to the work immediately and investigate your claim.

Article

Characterization of Flexor Digitorum Superficialis Muscle Stiffness Using Ultrasound Shear Wave Elastography and MyotonPRO: A Cross-Sectional Study Investigating the Correlation between Different Approaches

Phongpan Tantipoon ^{1,2} , Nuttaporn Praditpod ², Markus Pakleppa ¹, Chunhui Li ^{1,*} and Zhihong Huang ¹

¹ Biomedical Engineering, School of Science and Engineering, University of Dundee, Dundee DD1 4HN, UK; ptantipoon@dundee.ac.uk (P.T.); m.z.pakleppa@dundee.ac.uk (M.P.); z.y.huang@dundee.ac.uk (Z.H.)

² Department of Physical Therapy, Faculty of Allied Health Science, Thammasat University, Bangkok 12120, Thailand; nuttaporn.p@allied.tu.ac.th

* Correspondence: c.li@dundee.ac.uk

Abstract: Muscle stiffness provides a key insight toward clinical assessment for rehabilitation. Regarding the high-cost and technical skill requirement of ultrasound shear wave elastography (SWE) restricting extensive clinical use, MyotonPRO has been proposed as a complementary tool for muscle stiffness measurement. There is a deficiency of studies revealing the use of this tool for measuring muscle stiffness contributing to hand control. The purpose of this study was to assess the capability and effectiveness of MyotonPRO and SWE for hand muscle stiffness characterization. The stiffness of the dominant flexor digitorum superficialis (FDS) muscle of 25 healthy participants (12 males and 13 females) aged 29.60 ± 9.81 years was evaluated while they performed grip tasks. The muscle stiffness of males and females was compared. The correlation between dynamic muscle stiffness given by MyotonPRO and Young's modulus obtained from SWE was investigated. Statistical analysis indicated a significant difference in the dynamic muscle stiffness between genders in all conditions ($p < 0.05$), whereas a significant difference in Young's modulus was found only at the resting state. A moderate correlation was found between dynamic muscle stiffness and Young's modulus (r ranged from 0.243 to 0.489). Therefore, MyotonPRO can be used to assess the muscle stiffness of the FDS muscle at rest and during muscle contraction.

Keywords: ultrasonography; elastography; diagnostic imaging; elastic modulus; hand muscle; MyotonPRO



Citation: Tantipoon, P.; Praditpod, N.; Pakleppa, M.; Li, C.; Huang, Z. Characterization of Flexor Digitorum Superficialis Muscle Stiffness Using Ultrasound Shear Wave Elastography and MyotonPRO: A Cross-Sectional Study Investigating the Correlation between Different Approaches. *Appl. Sci.* **2023**, *13*, 6384. <https://doi.org/10.3390/app13116384>

Academic Editor: Silvestro Roatta

Received: 20 April 2023

Revised: 18 May 2023

Accepted: 22 May 2023

Published: 23 May 2023



Copyright: © 2023 by the authors. Licensee MDPI, Basel, Switzerland. This article is an open access article distributed under the terms and conditions of the Creative Commons Attribution (CC BY) license (<https://creativecommons.org/licenses/by/4.0/>).

1. Introduction

Muscle stiffness is one of the mechanical properties of skeletal muscle that is recognized as a marker of muscle performance and joint stability during the operation of functional movements [1,2]. The flexor digitorum superficialis (FDS) muscle is an important muscle involved in finger movement and grip strength [3,4]. Alterations in the stiffness of the FDS muscle have been noticed in neuromuscular pathology [5–7]. Moreover, this parameter can be used for examining the process of muscle recovery from hand injuries [8–11] or adaptation owing to exercise [12–14]. Therefore, exploring FDS muscle stiffness would provide key insight into clinical assessment [12,15] and the design of assistive technologies and strategies for hand rehabilitation [16,17].

Ultrasound shear wave elastography (SWE) has been developed for the direct measurement of the mechanical properties of the muscle. This approach is able to offer a non-invasive and reliable tool for characterizing muscle stiffness [18–20]. Shear waves are generated into the tissue by acoustic radiation force, and then the velocity of wave propagation is estimated and used for elasticity calculation [19,21–23]. Most previous

studies have emphasized measuring the stiffness of the musculotendinous structures of the lower extremities in the context of sports medicine [24–27] and certain diseases [28–31]. On the other hand, a few research studies applying the method to the upper limb muscles have been reported [32–35]. However, assessing the stiffness of the muscle contributing to hand function and dexterity is currently less well-established [36–38]. Moreover, flexor digitorum superficialis (FDS) muscle stiffness has never been investigated within quantitative SWE [7]. In the meantime, most studies have underlined reporting the normative data of resting muscle stiffness, and the quantification of muscle stiffness during muscle contraction has been constrained [18,19,39–42]. However, there are some limitations of SWE for clinical use, including its high-cost and technical skill requirement [23,43,44].

Recently, MyotonPRO (Myoton AS, Estonia) has been proposed as a portable, non-invasive, painless, and reliable tool for measuring the mechanical properties of the muscle [45,46]. It is a handheld digital palpation device equipped with a muscle stiffness measurement function. Once the measurement has been performed, the damped natural oscillation of the biological tissue is recorded as a form of the acceleration signal. Subsequently, the simultaneous computation of the related parameters is evaluated [47,48]. Previous studies have revealed excellent intra- and inter-tester reliability of the device for measuring the mechanical properties of the muscle. Therefore, MyotonPRO is a feasible alternative tool for quantifying muscle stiffness in different conditions [49,50]. However, only a few studies have reported using MyotonPRO to evaluate the upper limb muscles [47,51,52]. Currently, studies assessing how the stiffness of the muscle contributes to hand control using this device have not been reported. However, there is a deficiency of studies that have revealed the capability and effectiveness of MyotonPRO for measuring hand muscle stiffness compared to SWE. Therefore, it remains to be seen whether MyotonPRO and SWE can be used to evaluate FDS muscle stiffness and what the relationship between the muscle stiffness obtained from the different approaches is.

Therefore, the primary purpose of this study was to assess the capability and effectiveness of MyotonPRO and SWE for FDS muscle stiffness characterization. The second purpose was to investigate the correlation between the muscle stiffness achieved from the two different approaches in order to confirm that MyotonPRO could be used as a complementary tool for muscle stiffness measurement instead of SWE. We hypothesized that MyotonPRO and SWE could be used to assess the muscle stiffness of the FDS muscle at rest and during muscle contraction. Furthermore, we hypothesized that the dynamic muscle stiffness obtained from MyotonPro and Young's modulus achieved from SWE would have a positive correlation.

2. Materials and Methods

2.1. Study Design

This study was designed as a cross-sectional study. The study was divided into two sessions: the measurement of muscle stiffness using SWE and MyotonPRO [19,47]. The flexor digitorum superficialis (FDS) muscle of the dominant hand was chosen as being representative of the hand muscle owing to it being considered the key extrinsic muscle that contributes to hand function [53]. Handgrip was used to investigate muscle function. The muscle stiffness of the FDS was evaluated at both the resting state and during muscle contraction. The maximum voluntary contraction (MVC) of the FDS muscle was examined and used to determine the different intensities of muscle contraction forces. The intensity of muscle contraction was divided into five different levels 0%, 20%, 40%, 60%, and 80%MVC, and these were determined using a digital grip dynamometer [54,55].

2.2. Sample Size

A statistical power analysis was performed for sample size estimation using G*Power Version 3.1.9.7, based on the preliminary data of dynamic stiffness of the muscle difference from a sample of 10 participants. The effect size in this study was 1.3. With an alpha = 0.05 and power = 0.80, the projected total sample size required with this effect size

was 20 participants for 2 groups (10 for each group). Therefore, the sample size that was used in this study was 25 (12 males and 13 females).

2.3. Participants and Setting

The study was carried out in an ultrasound laboratory at Ninewells Hospital between October 2022 and December 2022. Twenty-five healthy participants (12 males and 13 females) aged from 18 to 60 years were recruited for the study. They did not have either a family history or a history of neurological or psychiatric disorders, or a history of substance abuse. Participants were excluded from the study if they had a BMI greater than 30 kg/m², as it would have an adverse effect on obtaining good-quality ultrasound images [56]. In addition, participants were excluded from the study if they had any impairments or problems that might affect the experimental protocols, including a history of neuromuscular disease or musculoskeletal injury, surgery in the previous six months, surgical implant placement on upper limbs, or any current pain in the neck and upper limbs. Participants' handedness was assessed using the Edinburgh inventory questionnaire [57]. Twenty-one participants were right-handed, two participants were left-handed, and another two were ambidextrous. A participant information sheet was provided, and a consent form was signed by all the participants prior to the data collection process. This study was approved by the School of Science and Engineering Research Ethics Committee (SSEREC), University of Dundee.

2.4. Measurements

2.4.1. Ultrasound Shear Wave Elastography (SWE) Measurement

SWE measurements were carried out using the Verasonics research system (Vantage 128 TM, Verasonics Inc., Kirkland, WA, USA) and linear array transducer with a central frequency of 5.2 MHz (L7-4, Philips Healthcare, Andover, MA, USA). The focused comb-push ultrasound shear elastography (F-CUSE) approach proposed by Song et al. (2018) was applied in this study [58]. The Verasonics research system and L7-4 transducer were used to generate comb-push beams and track shear wave motion. The setup script for the data acquisition was modified in accordance with the F-CUSE principle. A single push-detection data acquisition triggered multiple sources of distribution of shear waves in tissue concurrently. Therefore, a total of 128 elements of the transducer were divided equally into four subgroups. A 4-tooth focused comb-push (32 elements for each push beam) transmitted focused ultrasound push beams simultaneously. The push duration for each beam was 600 µs. Multiple laterally distributed sources of the shear wave were then developed. Each push beam created two shear waves propagating in opposing directions, far away from the push beam, and then the waves from the different push beams interfered with each other and eventually filled the entire full field of view.

Once the transmission was completed, the system instantaneously switched to plane wave imaging mode with all transducer elements. The plane-wave imaging compounding method was used to improve the signal-to-noise ratio (SNR) of shear wave tracking. Three frames at three different steering angles (-4° , 0° , 4°) were used to achieve one imaging frame. Shear wave velocity was calculated from axial particle velocity (V_z) induced by the propagation of the shear wave. The V_z was computed from the in-phase/quadrature (IQ) data of consecutive frames using a 1D autocorrelation method. A directional filter was used to eliminate destructive shear wave interferences. Local shear wave velocity was recovered by the time-of-flight algorithm by cross-correlating particle velocity profiles along the lateral direction. The elasticity map was then reconstructed [59–61].

2.4.2. MyotonPRO Measurement

Muscle stiffness was measured using a novel hand-help digital palpation device, namely the MyotonPRO (Myoton AS, Tallinn, Estonia). The standard 3 mm diameter probe was positioned perpendicularly to the skin surface over the target muscle. The device provided an automatic pre-compression of 0.18 N to the target area (total duration of 400 ms) in order to allow for the registration of the natural damping oscillation of the muscle

through the overlaid skin and subcutaneous tissue. A light quick-release mechanical force of 0.4 N was then applied for 15 ms to induce deformation of the muscle. The muscle will then respond to the exterior mechanical impulse by a damped natural oscillation caused by its viscoelastic properties. The oscillations are recorded by a built-in accelerometer at a sampling rate of 3200 Hz and then shown in the form of an acceleration graph [51,62].

2.5. Procedures

The location of the flexor digitorum superficialis (FDS) muscle was based on the anatomical landmarks and palpation. Participants were seated upright comfortably while their arms rested on the table. The elbow was bent approximately 90° of flexion, the forearm was supinated, the hand was palm up, and the wrist and fingers were relaxed. The area between the tendon of the palmaris longus and the flexor carpi ulnaris was palpated while the forearm was relaxed. Subsequently, the participant was asked to flex the middle and ring fingers with maximum force, and the researcher determined where the maximum displacement occurred on the muscle belly; normally, this will be at the midpoint of the distance between the medial epicondyle of the humerus and styloid process of the ulna. Finally, this area was marked by a non-permanent marker as a rectangular shape, approximately a dimension of 1 cm × 4.5 cm (width × length), to use as the marked point for transducer placement during ultrasound scanning (Figure 1A).

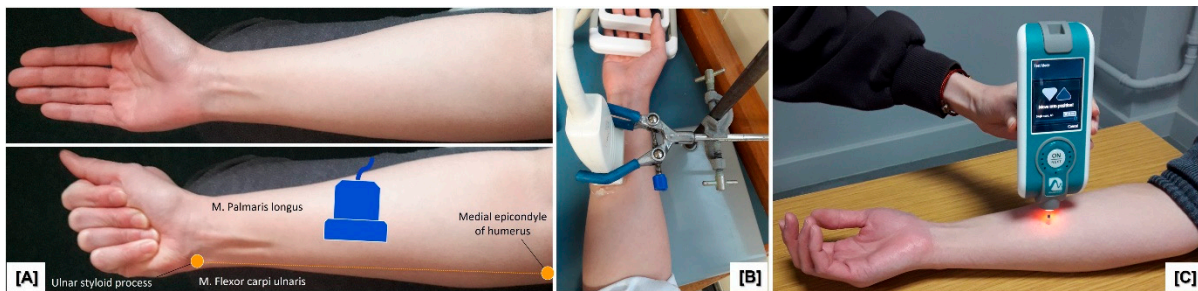


Figure 1. Experimental set up; (A) FDS muscle landmark determination, (B) Setup for SWE measurement and (C) Set up for MyotonPRO measurement.

For the next step, individual maximum grip force was evaluated using a digital grip dynamometer (CAMRY-EH101, Zhongshan Camry Electronic Co, Ltd., Zhongshan, Guangdong, China) to achieve the maximum voluntary contraction of the FDS muscle (100%MVC), which was used for further determining the different intensities of maximum voluntary contraction (%MVC). Once the 100%MVC was obtained, %MVC was estimated and defined as 0%, 20%, 40%, 60% and 80%MVC. Subsequently, the participant was given time to practice the required task of data acquisition. They were asked to grasp the grip dynamometer until the force reached the target value of all different %MVC and they could maintain the target force level for a while.

Once the skill to perform different levels of grasping was achieved, SWE measurement began. The participant was in the aforementioned position and relaxed their forearm and hand. The transducer coated with ultrasound gel was positioned on a custom holder to maintain a fixed position and then placed over the marked point with firm and minimal contact pressure. The alignment of the probe was adjusted to be perpendicular to the skin surface and parallel to the direction of the muscle fibres (Figure 1B). For data acquisition, the structural image of the dominant FDS muscle in five different %MVC was acquired. First, scanning began to obtain the structure image of the muscle in a resting condition (0%MVC). The participant was then instructed to grasp the grip dynamometer with different force levels of 20%, 40%, 60% and 80%MVC randomly, to avoid any potential source of bias. Each level of grasping was maintained for 10 s. The procedure was repeated in two trials for each subject with two minutes of rest period between force levels holds and trials. The average value from these two trials was used for further data analysis.

Once the SWE measurement was completed, the participant received a 10 min rest to achieve the baseline relaxation state of the muscle before continuing with the MyotonPRO measurement. The participant was asked to be in the same position; the centre of the ultrasound scanning landmark was marked as cross-shaped for use as the location of the measurement. The tip of the device's probe was placed perpendicular to the marked site (Figure 1C). Subsequently, the participant was instructed to grasp the grip dynamometer with different force levels of 20%, 40%, 60% and 80%MVC randomly in order to avoid any potential source of bias. Each level of grasping was maintained for 10 s. The procedure was repeated in two trials for each subject with two minutes of rest period between force levels holds and trials. The average value from these two trials was used for further data analysis.

2.6. Data Analysis

2.6.1. Young's Modulus Estimation

Once the data acquisition of the SWE measurement was completed, the requisite parameters were exported for data processing through MATLAB script (Mathworks, Natick, MA, USA). The boundary of the FDS muscle was outlined, and then a $10 \times 30 \text{ mm}^2$ region of interest (ROI) was defined within the muscle layer. The elasticity map was reconstructed, and the shear wave velocity (V_s) was extracted from the map.

Afterwards, the shear wave velocity (V_s) was used for muscle elasticity calculation. As V_s is proportional to the shear modulus of the muscle (μ ; in a unit of kPa), μ can be calculated by the equation as follows:

$$\mu = \rho V_s^2 \quad (1)$$

where ρ is the density of muscle (1000 kg/m^3). Regarding skeletal muscle being heterogeneous and/or anisotropic material, the V_s can be basically used as a reliable surrogate for the stiffness of the tissue [63,64].

However, previous studies have revealed that muscle shear modulus (μ) has a strong linear relationship with Young's modulus (E ; in a unit of kPa) when the scanning plane is aligned parallel to the muscle fibre direction [14]. Subsequently, the muscle is supposed to be isotropic, uniform and has quasi-incompressible characteristics, so μ is directly related to E . Therefore, E can be obtained from the equation as follows:

$$E = 3\mu \quad (2)$$

or

$$E = 3\rho V_s^2 \quad (3)$$

Consequently, the value of E could be used for estimating the stiffness of the FDS muscle in this study [19,21,65].

2.6.2. Dynamic Stiffness Calculation

From the MyotonPRO measurement, the acceleration graph was provided. Dynamic stiffness of the muscle (S) is represented as a characterization of the resistance of biological soft tissues to a force of deformation, so S can be calculated by the equation as follows:

$$S = a_{max} \cdot m_{probe} / \Delta l \quad (4)$$

When a_{max} is the maximum acceleration of the damped oscillation, which characterizes the biological tissue resistance to deformation force caused by an external force, m_{probe} is the mass of the measurement mechanism, and Δl is the maximum displacement point of the tissue [66].

2.7. Statistical Analysis

Statistical analysis was performed using IBM SPSS Statistics 26. The normality of data distribution was tested using the Kolmogorov–Smirnov test. The independent-sample

t-test was used to compare mean age, weight, height and BMI between males and females as the data were normally distributed. On the other hand, the mean Young's modulus and the dynamic muscle stiffness of different %MVCs between males and females were non-normally distributed, so the independent-sample Mann–Whitney U test was used for the statistical analysis. The correlations between the muscle stiffness of all the participants, measured by MyotonPRO and SWE, were investigated using Pearson's correlation analysis. The statistical significance was set at $p < 0.05$.

3. Results

Twenty-five healthy participants (12 males and 13 females) with ages of 29.60 ± 9.81 years, height 1.69 ± 0.09 m, weight 65.85 ± 14.76 kg, and BMI 22.65 ± 3.53 kg/m² participated in the study. The demographics of the participants are shown in Table 1.

Table 1. General characteristic of participants.

	Total ($n = 25$)	Males ($n = 12$)	Females ($n = 13$)	<i>p</i> -Value
Age (years)	29.60 ± 9.81	27.92 ± 5.53	31.15 ± 12.73	0.017 *
Weight (kg)	65.85 ± 14.76	73.67 ± 14.62	58.63 ± 11.04	0.915
Height (m)	1.69 ± 0.10	1.76 ± 0.07	1.62 ± 0.06	0.101
BMI (kg/m ²)	22.95 ± 3.53	23.61 ± 3.35	22.34 ± 3.71	0.899

Abbreviation: kg—kilogram; m—metre; kg/m²—kilograms per square meter; BMI—body mass index. * Independent-samples *t*-test, *p*-value < 0.05.

From the SWE measurements, elasticity maps of the FDS muscle in different intensities of muscle contraction are shown in Figure 2. For males, the mean Young's modulus of the resting state (0%MVC) was 35.86 ± 8.74 kPa. When grasping intensity was changed to 20%, 40%, 60% and 80%MVC, there was an alteration in the level of muscle activation; mean Young's modulus was 55.92 ± 14.73 , 70.00 ± 11.81 , 85.15 ± 18.95 and 103.79 ± 17.76 kPa, respectively. In the case of females, the mean Young's modulus of the resting state (0%MVC) was 27.47 ± 5.59 kPa. When grasping intensity increased to 20%, 40%, 60%MVC and 80%MVC, the mean Young's modulus was 47.91 ± 16.76 , 63.16 ± 19.26 , 80.82 ± 19.67 and 102.39 ± 20.36 kPa, respectively. The results of this study revealed that the mean Young's modulus for different intensities of muscle contraction in males was significantly higher than in females (Table 2). The statistical analyses indicated that there were significant differences ($p < 0.05$) between the mean Young's modulus of males and females at only 0%MVC. However, there were no significant differences in the muscle elasticity at 20%, 40%, 60% and 80%MVC (Figure 3).

From the MyotonPRO measurements, the results of this study revealed that the mean dynamic muscle stiffness in different intensities of muscle contraction in males was significantly higher than in females, as shown in Table 2. For males, the mean resting dynamic muscle stiffness (0%MVC) was 355.46 ± 26.07 kPa. When muscle activation increased to 20%, 40%, 60% and 80%MVC, the mean dynamic muscle stiffness also increased to 442.96 ± 50.12 , 522.58 ± 53.04 , 566.63 ± 62.74 and 603.63 ± 70.70 kPa, respectively. For females, the mean resting dynamic muscle stiffness (0%MVC) was 303.54 ± 45.66 kPa. When the intensity of grasping increased to 20%, 40%, 60% and 80%MVC, the mean dynamic muscle stiffness was 371.12 ± 57.99 , 398.81 ± 138.15 , 464.69 ± 90.46 and 497.73 ± 98.25 kPa, respectively. The statistical analyses indicated that there were significant differences ($p < 0.05$) between the mean dynamic muscle stiffness of males and females at all different intensities of muscle contraction (Figure 4).

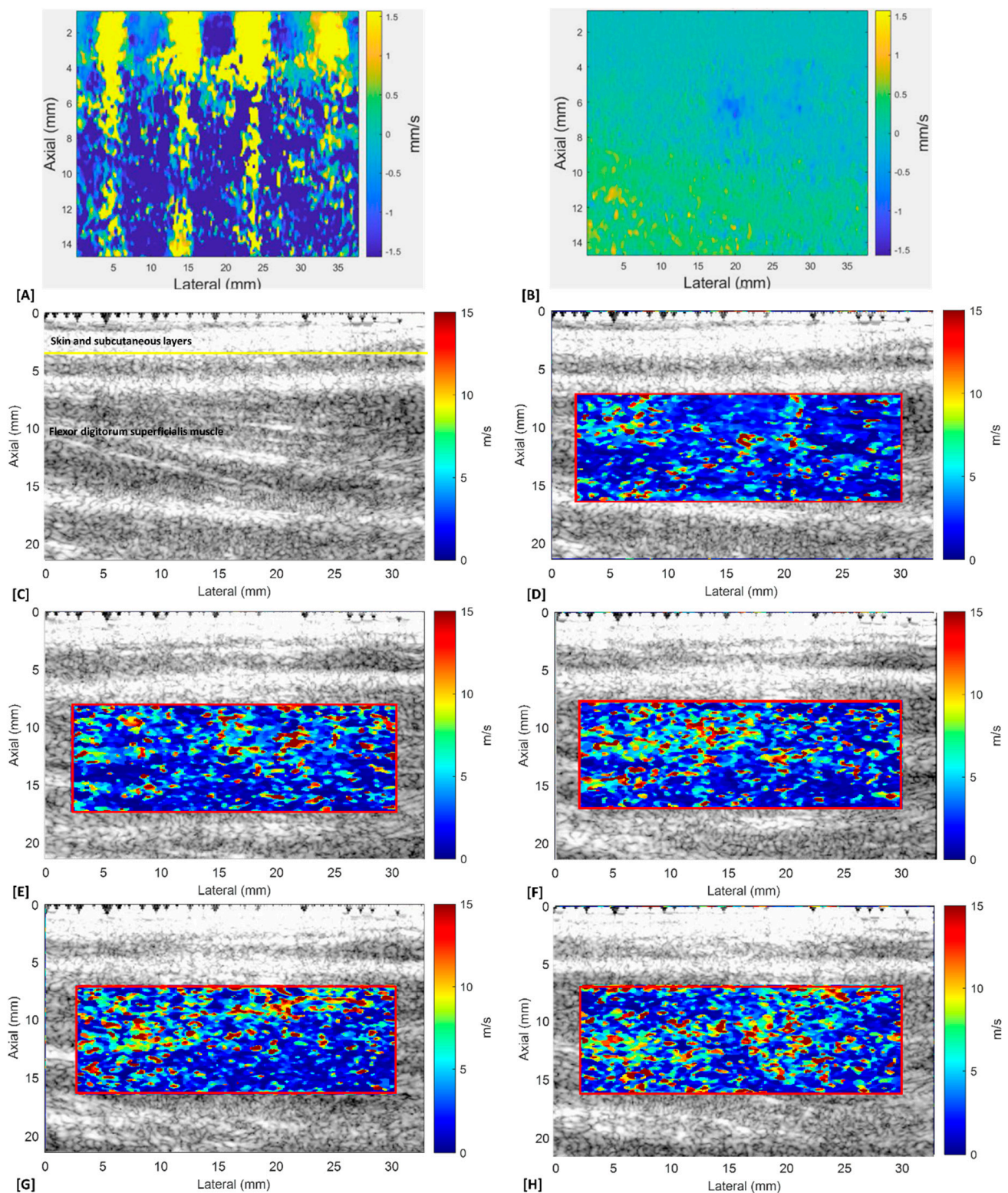
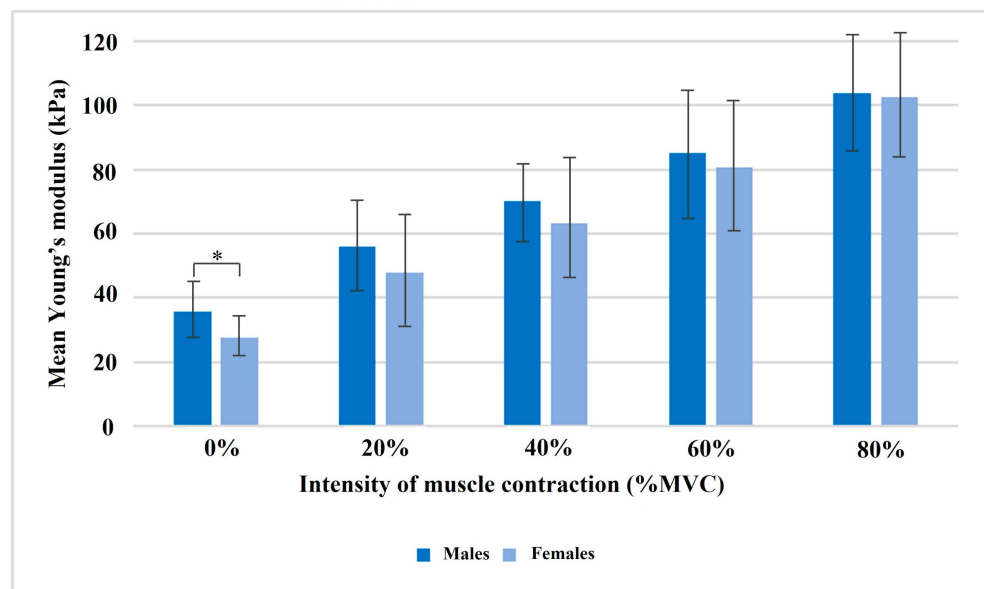


Figure 2. Representative shear wave elastography image for the evaluation of flexor digitorum superficialis (FDS) muscle stiffness in different intensities of muscle contraction. (A,B) Motion (particle velocity in an axial direction) distribution at T1 and T2, respectively. (C) Structural image shows the target layer of the FDS muscle. (D–H) Elasticity map in the muscle at 0%, 20%, 40%, 60% and 80%MVC, respectively. The result revealed that muscle stiffness increases at higher intensity of muscle contraction.

Table 2. Mean Young’s modulus and dynamic muscle stiffness of FDS in different intensity of muscle contraction.

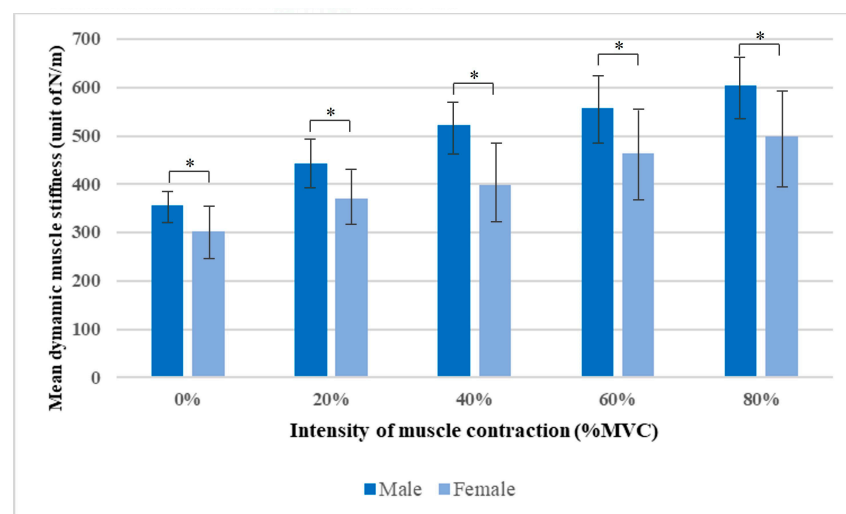
	0%MVC	20%MVC	40%MVC	60%MVC	80%MVC
Young’s modulus (kPa):					
Male	35.86 ± 8.74	55.92 ± 14.73	70.00 ± 11.81	85.15 ± 18.95	103.79 ± 17.76
Female	27.47 ± 5.59	47.91 ± 16.76	63.16 ± 19.26	80.82 ± 19.67	102.39 ± 20.36
<i>p</i> -value	0.010 *	0.168	0.247	0.769	0.728
Dynamic muscle stiffness (N/m):					
Male	355.46 ± 26.07	442.96 ± 50.12	522.58 ± 53.04	556.63 ± 62.74	603.63 ± 70.70
Female	303.54 ± 45.66	371.12 ± 57.99	398.81 ± 88.15	464.69 ± 90.46	497.73 ± 98.25
<i>p</i> -value	0.005 *	0.005 *	<0.001 *	0.002 *	0.007 *

Abbreviation: MVC—maximum voluntary contraction; kPa—kilopascal; N/m—newton metre * Independent-samples Mann-Whitney U test, *p*-value < 0.05.



* Independent-samples Mann-whitney U test, *p* < 0.05

Figure 3. Mean Young’s modulus of the flexor digitorum superficialis (FDS) muscle at different intensities of muscle contraction.



* Independent-samples Mann-whitney U test, *p* < 0.05

Figure 4. Mean dynamic muscle stiffness of the flexor digitorum superficialis (FDS) muscle at different intensities of muscle contraction.

In terms of the relationship between dynamic muscle stiffness given by MyotonPRO and Young's modulus obtained from SWE, there was a moderate direct correlation between the values at all %MVC levels, as shown in Table 3. Statistical analysis indicated that there was a significant correlation between the muscle stiffness value at the 0%MVC and 40%MVC levels. However, a significant difference was not found at the remaining levels, that is, at 20%, 60% and 80%MVC.

Table 3. Correlation coefficients (R) of Young's modulus and dynamic muscle stiffness of in different intensity of muscle contraction ($n = 25$).

	Young's Modulus (kPa):	Dynamic Muscle Stiffness (N/m):	R	p-Value
0%MVC	31.50 ± 8.30	328.46 ± 45.33	0.489	0.013 *
20%MVC	51.76 ± 16.02	405.60 ± 64.61	0.366	0.072
40%MVC	66.44 ± 16.17	458.22 ± 121.72	0.479	0.015 *
60%MVC	82.90 ± 19.05	508.82 ± 89.96	0.330	0.107
80%MVC	103.07 ± 18.77	548.56 ± 100.17	0.243	0.242

Abbreviation: MVC—maximum voluntary contraction; kPa—kilopascal; N/m—newton metre. * Pearson's correlation analysis, p -value < 0.05.

4. Discussion

The purpose of the present study was to assess the capability and effectiveness of MyotonPRO and SWE for the characterization of the flexor digitorum superficialis (FDS), which is the key muscle that contributes to the movement of the hand, especially the grasping task. The mechanical properties of skeletal muscle, including passive and active contraction properties, are essential for performing the function of the muscle. Therefore, FDS passive and active muscle stiffness was measured using ultrasound shear wave elastography (SWE) and MyotonPRO, both at rest (0%MVC) and during muscle contraction (20%, 40%, 60% and 80%MVC), respectively. The muscle stiffness values of males and females were compared in order to achieve key insight into the optimal value of the hand muscle in healthy subjects at different conditions of muscle activation. In addition, a correlation between the muscle stiffness value achieved from two different approaches was investigated to identify whether MyotonPRO can be used for assessing muscle stiffness compared to SWE.

The flexor digitorum superficialis (FDS) muscle is considered to be one of the key muscles that controls the movement of the hand. It is the largest extrinsic muscle of the hand, located in the anterior compartment of the forearm. Although this muscle forms as the intermediate muscle layer between the superficial and deep muscle groups of the forearm, its muscle belly is close to the surface of the forearm. Therefore, the activation level of this muscle is relatively straightforward to record and analyse [53,67]. Although some previous studies have emphasized the measurement of muscle stiffness in the upper extremities using ultrasound shear wave elastography [41,68–70], the evaluation of the stiffness of the muscle of the hand is currently less well established [1,36,37,71]. Therefore, the task in the present study has advantages over previous studies owing to the focus on the evaluation of the muscle stiffness of the FDS muscle.

From the measurement of muscle stiffness using SWE and MyotonPRO, the results of this study showed that the muscle stiffness of the FDS muscle increased when the intensity of muscle contraction was increased from 0%MVC to 80%MVC. Previous studies state that the magnitude of the mechanical changes with contraction is positively and linearly correlated with muscle force [20,70]. The increment in the elasticity during muscle activation is possible because of the rising number of attached cross-bridges of actin and myosin filaments during the cross-bridges cycle [41,72].

The present study found that there were significant differences ($p < 0.05$) between the mean Young's modulus of males and females only at the resting condition of the muscle. However, there were no significant differences in the muscle elasticity during muscle contraction, at 20%, 40%, 60% or 80%MVC. SWE measurement relies on the principle

that soft tissues are purely elastic, incompressible and isotropic. Therefore, the major factor that affected the results of this study was the anisotropic physical properties of the skeletal muscle, as the skeletal muscle consists of a parallel arrangement of myofibrils, muscular fibres, collagen and elastic fibres, and fascicles that result in its anisotropic action [19,21,63,64].

Furthermore, muscle stiffness measurements are sensitive to the angle between the axis of the transducer and the orientation of the muscular fibres. Young's modulus is correlated with shear modulus only if the transducer is oriented parallel to the muscle fibres. The propagation of shear waves along the direction of the fibres is faster than the perpendicular one. In addition, the pennation angle of the muscle is also changed once the muscle is in different contraction conditions. Therefore, the relationship between the orientation of the transducer and muscle fibre direction may have affected the results of this study, especially when measured during voluntary contraction [19,73].

During voluntary contraction, the muscle will become stiffer. Propagation of the shear wave in more rigid tissue is too fast to be detected for some ultrasound systems. Consequently, the stiffness value at the greater contraction of the muscle, which is nearly the level of maximum voluntary contraction, cannot be evaluated [19]. Currently, for the measurement of active muscle stiffness using an ultrasound elastography approach, the level of muscle contraction has been analysed only at a sub-maximum voluntary contraction of about 40%–70%MVC [18,36,74].

On the one hand, the MyotonPRO measurement showed a significant difference ($p < 0.05$) between the mean dynamic muscle stiffness of males and females, both when resting and at all levels of muscle contraction. These results also support previous studies that suggest MyotonPRO can be used to detect different conditions of muscle contraction, which are theorized to reflect varying conditions of stiffness during functional activities. MyotonPRO has demonstrated the ability to discriminate between different muscle contraction intensities [47,51,52]. In addition, in this research, there was a moderate positive correlation between dynamic muscle stiffness and Young's modulus. Therefore, MyotonPRO can be used as an alternative measurement to assess the muscle stiffness of the FDS muscle at rest and during muscle contraction.

The potential limitations of this study are addressed. Firstly, the resting and contracting states of the muscle were not monitored using electromyography; instead, they were determined by a hand grip dynamometer. Accurately investigating the resting state of the muscle and the occurrence of muscle fatigue during data-gathering processes was challenging. Therefore, EMG could be combined for further study to monitor muscle activity. Secondly, the subcutaneous fat thickness has not been measured before to measure muscle stiffness using MyotonPRO and SWE. In this respect, MyotonPRO is not suitable for measuring muscle stiffness once muscles are covered with subcutaneous fat of more than 20 mm. Therefore, further studies should measure subcutaneous fat to control this covariate. Thirdly, a small sample size was used in this study, and the effect of age was not considered. A relatively wide range of ages of participants, varying from 18 to 60 years, could potentially encompass considerably different mechanical properties of the muscle; therefore, these could be considered for further study. Furthermore, this study focused only on healthy subjects, so further studies should include different types of subjects, such as athletes or people with neuromuscular problems, in order to compare and generalize the results for each population.

5. Conclusions

The results revealed a moderate correlation between dynamic muscle stiffness achieved from MyotonPRO measurement and Young's modulus obtained from SWE measurement. There was a significant difference in the dynamic muscle stiffness between males and females ($p < 0.05$) at all conditions of muscle contraction. In contrast, a significant difference in Young's modulus was found only at the resting state. Therefore, the present study revealed that MyotonPRO can be used in FDS muscle stiffness measurement, at rest and

during muscle contraction. This could be an alternative option to solve the limitations of using ultrasound to measure muscle stiffness in clinics. However, caution is warranted in clinical settings when applying it to other muscles, populations, and age groups, and in different conditions.

Author Contributions: Supervision, M.P., C.L. and Z.H.; Conception and design of the study, P.T., M.P., C.L., Z.H. and N.P.; Methodology, P.T., M.P., C.L., Z.H. and N.P.; Data acquisition and data analysis, P.T. and N.P.; Data interpretation, P.T., M.P., C.L. and N.P.; Writing—Original Draft Preparation, P.T. and N.P.; Writing—Review and Editing, P.T., N.P., C.L. and M.P. All authors have read and agreed to the published version of the manuscript.

Funding: This research received no external funding.

Institutional Review Board Statement: The study was conducted in accordance with the Declaration of Helsinki and approved by the School of Science and Engineering Research Ethics Committee (SSEREC), the University of Dundee (UOD-SSEREC-MSc-TPG-2019-037, approved on 17 October 2022).

Informed Consent Statement: Informed consent was obtained from all subjects involved in the study.

Data Availability Statement: The data are available from the corresponding author upon reasonable request.

Acknowledgments: The authors would like to thank staff and PhD students in Biomedical Engineering, School of Science and Engineering, University of Dundee and all of the participants for their support in this study.

Conflicts of Interest: The authors declare no conflict of interest.

References

1. Bilston, L.E.; Tan, K. Measurement of passive skeletal muscle mechanical properties in vivo: Recent progress, clinical applications, and remaining challenges. *Ann. Biomed. Eng.* **2015**, *43*, 261–273. [[CrossRef](#)] [[PubMed](#)]
2. Needle, A.R.; Baumeister, J.; Kaminski, T.W.; Higginson, J.S.; Farquhar, W.B.; Swanik, C.B. Neuromechanical coupling in the regulation of muscle tone and joint stiffness. *Scand. J. Med. Sci. Sports* **2014**, *24*, 737–748. [[CrossRef](#)] [[PubMed](#)]
3. Nordin, M.; Frankel, V.H. (Eds.) *Basic Biomechanics of the Musculoskeletal System*; Lippincott Williams & Wilkins: New York, NY, USA, 2001.
4. Oatis, C.A. *Kinesiology: The Mechanics and Pathomechanics of Human Movement*; Lippincott Williams & Wilkins: Baltimore, MD, USA, 2009.
5. Ferreira-Sánchez, M.D.R.; Moreno-Verdú, M.; Cano-de-La-Cuerda, R. Quantitative measurement of rigidity in Parkinson's disease: A systematic review. *Sensors* **2020**, *20*, 880. [[CrossRef](#)] [[PubMed](#)]
6. Faturi, F.M.; Santos, G.L.; Ocamoto, G.N.; Russo, T.L. Structural muscular adaptations in upper limb after stroke: A systematic review. *Top. Stroke Rehabil.* **2019**, *26*, 73–79. [[CrossRef](#)] [[PubMed](#)]
7. Kenis-Coskun, O.; Giray, E.; Gencer-Atalay, Z.K.; Yagci, I.; Karadag-Saygi, E. Reliability of quantitative ultrasound measurement of flexor digitorum superficialis and profundus muscles in stroke. *J. Comp. Eff. Res.* **2020**, *9*, 1293–1300. [[CrossRef](#)] [[PubMed](#)]
8. Simon, A.M.; Turner, K.L.; Miller, L.A.; Dumanian, G.A.; Potter, B.K.; Beachler, M.D.; Hargrove, L.J.; Kuiken, T.A. Myoelectric prosthesis hand grasp control following targeted muscle reinnervation in individuals with transradial amputation. *PLoS ONE* **2023**, *18*, e0280210. [[CrossRef](#)]
9. Vu, P.P.; Vaskov, A.K.; Irwin, Z.T.; Henning, P.T.; Lueders, D.R.; Laidlaw, A.T.; Davis, A.J.; Nu, C.S.; Gates, D.H.; Cederna, P.S. A regenerative peripheral nerve interface allows real-time control of an artificial hand in upper limb amputees. *Sci. Transl. Med.* **2020**, *12*, eaay2857. [[CrossRef](#)]
10. Chen, P.-Y.; Yang, T.-H.; Kuo, L.-C.; Shih, C.-C.; Huang, C.-C. Characterization of Hand Tendons through High-Frequency Ultrasound Elastography. *IEEE Trans. Ultrason. Ferroelectr. Freq. Control* **2019**, *67*, 37–48. [[CrossRef](#)]
11. Maslow, J.I.; Posey, S.L.; Habet, N.; Duemmler, M.; Odum, S.; Gaston, R.G. Central Slip Reconstruction with a Distally Based Flexor Digitorum Superficialis Slip: A Biomechanical Study. *J. Hand Surg.* **2022**, *47*, 145–150. [[CrossRef](#)]
12. Kocur, P.; Piwińska, I.; Goliwaś, M.; Adamczewska, K. Assessment of myofascial stiffness of flexor digitorum superficialis muscles in rock climbers. *Acta Bioeng. Biomech.* **2021**, *23*, 23–31. [[CrossRef](#)]
13. Colomar, J.; Baiget, E.; Corbi, F. Influence of strength, power, and muscular stiffness on stroke velocity in junior tennis players. *Front. Physiol.* **2020**, *11*, 196. [[CrossRef](#)] [[PubMed](#)]
14. Vinstrup, J.; Calatayud, J.; Jakobsen, M.D.; Sundstrup, E.; Jørgensen, J.R.; Casaña, J.; Andersen, L.L. Hand strengthening exercises in chronic stroke patients: Dose-response evaluation using electromyography. *J. Hand Ther.* **2018**, *31*, 111–121. [[CrossRef](#)] [[PubMed](#)]

15. Waitayawinyu, T.; Numnate, W.; Boonyasirikool, C.; Niempoog, S. Outcomes of Endoscopic Carpal Tunnel Release with Ring Finger Flexor Digitorum Superficialis Opponensplasty in Severe Carpal Tunnel Syndrome. *J. Hand Surg.* **2019**, *44*, 1095.e1–1095.e7. [[CrossRef](#)] [[PubMed](#)]
16. Boser, Q.A.; Dawson, M.R.; Schofield, J.S.; Dziwenko, G.Y.; Hebert, J.S. Defining the design requirements for an assistive powered hand exoskeleton: A pilot explorative interview study and case series. *Prosthet. Orthot. Int.* **2020**, *45*, 161–169. [[CrossRef](#)] [[PubMed](#)]
17. Díez, J.A.; BlancoJosé, A.; Catalán, J.M.; Badesa, F.J.; Lledó, L.D.; García-Aracil, N. Hand exoskeleton for rehabilitation therapies with integrated optical force sensor. *Adv. Mech. Eng.* **2018**, *10*, 1687814017753881. [[CrossRef](#)]
18. Brandenburg, J.E.; Eby, S.F.; Song, P.; Zhao, H.; Brault, J.S.; Chen, S.; An, K.-N. Ultrasound Elastography: The New Frontier in Direct Measurement of Muscle Stiffness. *Arch. Phys. Med. Rehab.* **2014**, *95*, 2207–2219. [[CrossRef](#)]
19. Creze, M.; Nordez, A.; Soubeyrand, M.; Rocher, L.; Maître, X.; Bellin, M.F. Shear wave sonoelastography of skeletal muscle: Basic principles, biomechanical concepts, clinical applications, and future perspectives. *Skelet. Radiol.* **2018**, *47*, 457–471. [[CrossRef](#)]
20. Ryu, J.; Jeong, W.K. Current status of musculoskeletal application of shear wave elastography. *Ultrasonography* **2017**, *36*, 185–197. [[CrossRef](#)]
21. e Lima, K.M.M.; Júnior, J.F.S.C.; de Albuquerque Pereira, W.C.; de Oliveira, L.F. Assessment of the mechanical properties of the muscle-tendon unit by supersonic shear wave imaging elastography: A review. *Ultrasonography* **2018**, *37*, 3–15. [[CrossRef](#)]
22. Blank, J.; Blomquist, M.; Arant, L.; Cone, S.; Roth, J. Characterizing Musculoskeletal Tissue Mechanics Based on Shear Wave Propagation: A Systematic Review of Current Methods and Reported Measurements. *Ann. Biomed. Eng.* **2022**, *50*, 751–768. [[CrossRef](#)]
23. Davis, L.C.; Baumer, T.G.; Bey, M.J.; Van Holsbeeck, M.T. Clinical utilization of shear wave elastography in the musculoskeletal system. *Ultrasonography* **2019**, *38*, 2–12. [[CrossRef](#)] [[PubMed](#)]
24. Romer, C.; Czupajllo, J.; Zessin, E.; Fischer, T.; Wolfarth, B.; Lerchbaumer, M.H. Stiffness of Muscles and Tendons of the Lower Limb of Professional and Semiprofessional Athletes Using Shear Wave Elastography. *J. Ultrasound Med.* **2022**, *41*, 3061–3068. [[CrossRef](#)] [[PubMed](#)]
25. Friede, M.C.; Klauser, A.; Fink, C.; Csapo, R. Stiffness of the iliotibial band and associated muscles in runner's knee: Assessing the effects of physiotherapy through ultrasound shear wave elastography. *Phys. Ther. Sport* **2020**, *45*, 126–134. [[CrossRef](#)]
26. Mendes, B.; Firmino, T.; Oliveira, R.; Neto, T.; Infante, J.; Vaz, J.R.; Freitas, S.R. Hamstring stiffness pattern during contraction in healthy individuals: Analysis by ultrasound-based shear wave elastography. *Eur. J. Appl. Physiol.* **2018**, *118*, 2403–2415. [[CrossRef](#)] [[PubMed](#)]
27. Römer, C.; Czupajllo, J.; Zessin, E.; Fischer, T.; Wolfarth, B.; Lerchbaumer, M.H. Muscle and Tendon Stiffness of the Lower Limb of Professional Adolescent Soccer Athletes Measured Using Shear Wave Elastography. *Diagnostics* **2022**, *12*, 2453. [[CrossRef](#)]
28. Zhang, H.; Peng, W.; Qin, C.; Miao, Y.; Zhou, F.; Ma, Y.; Gao, Y. Lower Leg Muscle Stiffness on Two-Dimensional Shear Wave Elastography in Subjects with Medial Tibial Stress Syndrome. *J. Ultrasound Med.* **2022**, *41*, 1633–1642. [[CrossRef](#)]
29. Wang, Z.; Lyu, G.; Zhong, H.; Yan, L.; Xu, Z. Shear Wave Elastography for Detecting Calf Muscle Stiffness: An Effective Tool for Assessing Sarcopenia. *J. Ultrasound Med.* **2023**, *42*, 891–900. [[CrossRef](#)]
30. Yin, L.; Du, L.; Li, Y.; Xiao, Y.; Zhang, S.; Ma, H.; He, W. Quantitative Evaluation of Gastrocnemius Medialis Stiffness During Passive Stretching Using Shear Wave Elastography in Patients with Parkinson's Disease: A Prospective Preliminary Study. *Korean J. Radiol.* **2021**, *22*, 1841–1849. [[CrossRef](#)]
31. Guo, Y.; Li, X.M.; Zhang, H.; Lu, H.T.; Feng, B.; Wang, Y.Z. Application of Ultrasound Shear Wave Elastography in Rehabilitation Assessment of Triceps Surae and Achilles Tendon after Stroke. *Chin. J. Rehabil. Theory Pract.* **2020**, *12*, 753–756.
32. Ding, C.W.; Song, X.; Fu, X.Y.; Zhang, Y.C.; Mao, P.; Sheng, Y.J.; Yang, M.; Wang, C.S.; Zhang, Y.; Chen, X.F.; et al. Shear wave elastography characteristics of upper limb muscle in rigidity-dominant Parkinson's disease. *Neurol. Sci.* **2021**, *42*, 4155–4162. [[CrossRef](#)]
33. Analan, P.D.; Ozdemir, H. Assessment of Post-Stroke Biceps Brachialis Muscle Stiffness by Shear-Wave Elastography: A Pilot Study. *Muscles Ligaments Tendons J.* **2020**, *10*, 531–536. [[CrossRef](#)]
34. Mifune, Y.; Inui, A.; Nishimoto, H.; Kataoka, T.; Kurosawa, T.; Yamaura, K.; Mukohara, S.; Niikura, T.; Kokubu, T.; Akisue, T.; et al. Assessment of posterior shoulder muscle stiffness related to posterior shoulder tightness in college baseball players using shear wave elastography. *J. Shoulder Elb. Surg.* **2020**, *29*, 571–577. [[CrossRef](#)] [[PubMed](#)]
35. Dieterich, A.V.; Yavuz, U.Ş.; Petzke, F.; Nordez, A.; Falla, D. Neck Muscle Stiffness Measured with Shear Wave Elastography in Women with Chronic Nonspecific Neck Pain. *J. Orthop. Sport. Phys. Ther.* **2020**, *50*, 179–188. [[CrossRef](#)]
36. Ateş, F.; Hug, F.; Bouillard, K.; Jubeau, M.; Frappart, T.; Couade, M.; Bercoff, J.; Nordez, A. Muscle shear elastic modulus is linearly related to muscle torque over the entire range of isometric contraction intensity. *J. Electromyogr. Kinesiol.* **2015**, *25*, 703–708. [[CrossRef](#)]
37. Watanabe, Y.; Iba, K.; Taniguchi, K.; Aoki, M.; Sonoda, T.; Yamashita, T. Assessment of the Passive Tension of the First Dorsal Interosseous and First Lumbrical Muscles Using Shear Wave Elastography. *J. Hand Surg.* **2019**, *44*, 1092.e1–1092.e8. [[CrossRef](#)]
38. Shin, K.J.; Yi, J.; Hahn, S. Shear-wave elastography evaluation of thenar muscle in carpal tunnel syndrome. *J. Clin. Ultrasound* **2023**, *51*, 510–517. [[CrossRef](#)] [[PubMed](#)]
39. Bernabei, M.; Lee, S.S.M.; Perreault, E.J.; Sandercock, T.G. Shear wave velocity is sensitive to changes in muscle stiffness that occur independently from changes in force. *J. Appl. Physiol.* **2020**, *128*, 8–16. [[CrossRef](#)]

40. Herzog, W. The problem with skeletal muscle series elasticity. *BMC Biomed. Eng.* **2019**, *1*, 28. [[CrossRef](#)]
41. Wang, A.B.; Perreault, E.J.; Royston, T.J.; Lee, S.S. Changes in shear wave propagation within skeletal muscle during active and passive force generation. *J. Biomech.* **2019**, *94*, 115–122. [[CrossRef](#)]
42. Kozinc, Ž.; Šarabon, N. Shear-wave elastography for assessment of trapezius muscle stiffness: Reliability and association with low-level muscle activity. *PLoS ONE* **2020**, *15*, e0234359. [[CrossRef](#)]
43. Wang, X.; Zhu, J.; Gao, J.; Hu, Y.; Liu, Y.; Li, W.; Chen, S.; Liu, F. Assessment of ultrasound shear wave elastography within muscles using different region of interest sizes, manufacturers, probes and acquisition angles: An ex vivo study. *Quant. Imaging Med. Surg.* **2022**, *12*, 3227–3237. [[CrossRef](#)] [[PubMed](#)]
44. Romano, A.; Staber, D.; Grimm, A.; Kronlage, C.; Marquetand, J. Limitations of Muscle Ultrasound Shear Wave Elastography for Clinical Routine—Positioning and Muscle Selection. *Sensors* **2021**, *21*, 8490. [[CrossRef](#)] [[PubMed](#)]
45. Li, Y.-P.; Liu, C.-L.; Zhang, Z.-J. Feasibility of Using a Portable MyotonPRO Device to Quantify the Elastic Properties of Skeletal Muscle. *Experiment* **2022**, *28*, e934121-1. [[CrossRef](#)] [[PubMed](#)]
46. Milerská, I.; Lhotská, L.; Macaš, M. Biomechanical Parameters of Muscles, Objective Assessment Using MyotonPRO. In Proceedings of the 2018 IEEE International Conference on Bioinformatics and Biomedicine (BIBM), Madrid, Spain, 3–6 December 2018; pp. 1522–1525.
47. Bailey, L.; Samuel, D.; Warner, M.B.; Stokes, M. Parameters representing muscle tone, elasticity and stiffness of biceps brachii in healthy older males: Symmetry and within-session reliability using the MyotonPRO. *J. Neurol. Disord.* **2013**, *1*, 1–7. [[CrossRef](#)]
48. Schneider, S.; Peipsi, A.; Stokes, M.; Knicker, A.; Abeln, V. Feasibility of monitoring muscle health in microgravity environments using Myoton technology. *Med. Biol. Eng. Comput.* **2015**, *53*, 57–66. [[CrossRef](#)]
49. Liu, C.; Feng, Y.; Zhang, H.; Li, Y.; Zhu, Y.; Zhang, Z. Assessing the viscoelastic properties of upper trapezius muscle: Intra- and inter-tester reliability and the effect of shoulder elevation. *J. Electromyogr. Kinesiol.* **2018**, *43*, 226–229. [[CrossRef](#)]
50. Liu, C.L.; Li, Y.P.; Wang, X.Q.; Zhang, Z.J. Quantifying the Stiffness of Achilles Tendon: Intra- and Inter-Operator Reliability and the Effect of Ankle Joint Motion. *Experiment* **2018**, *24*, 4876–4881. [[CrossRef](#)]
51. Feng, Y.N.; Li, Y.P.; Liu, C.L.; Zhang, Z.J. Assessing the elastic properties of skeletal muscle and tendon using shear-wave ultrasound elastography and MyotonPRO. *Sci. Rep.* **2018**, *8*, 17064. [[CrossRef](#)]
52. Kelly, J.P.; Koppenhaver, S.L.; Michener, L.A.; Proulx, L.; Bisagni, F.; Cleland, J.A. Characterization of tissue stiffness of the infraspinatus, erector spinae, and gastrocnemius muscle using ultrasound shear wave elastography and superficial mechanical deformation. *J. Electromyogr. Kinesiol.* **2018**, *38*, 73–80. [[CrossRef](#)]
53. Madarshahian, S.; Latash, M.L. Effects of hand muscle function and dominance on intra-muscle synergies. *Hum. Mov. Sci.* **2022**, *82*, 102936. [[CrossRef](#)]
54. Höppner, H.; Große-Dunker, M.; Stillfried, G.; Bayer, J.; van der Smagt, P. Key insights into hand biomechanics: Human grip stiffness can be decoupled from force by co-contraction and predicted from electromyography. *Front. Neurobotics* **2017**, *11*, 17. [[CrossRef](#)] [[PubMed](#)]
55. Martin, J.A.; Ramsay, J.; Hughes, C.; Peters, D.M.; Edwards, M.G. Age and grip strength predict hand dexterity in adults. *PLoS ONE* **2015**, *10*, e0117598. [[CrossRef](#)] [[PubMed](#)]
56. Brahee, D.D.; Ogedegbe, C.; Hassler, C.; Nyirenda, T.; Hazelwood, V.; Morchel, H.; Patel, R.S.; Feldman, J. Body mass index and abdominal ultrasound image quality: A pilot survey of sonographers. *J. Diagn. Med. Sonogr.* **2013**, *29*, 66–72. [[CrossRef](#)]
57. Oldfield, R.C. The assessment and analysis of handedness: The Edinburgh inventory. *Neuropsychologia* **1971**, *9*, 97–113. [[CrossRef](#)] [[PubMed](#)]
58. Song, P.; Chen, S. Comb-push Ultrasound Shear Elastography. In *Ultrasound Elastography for Biomedical Applications and Medicine*; Wiley: Hoboken, NJ, USA, 2018; pp. 388–397.
59. Song, P.; Urban, M.W.; Manduca, A.; Zhao, H.; Greenleaf, J.F.; Chen, S. Comb-push Ultrasound Shear Elastography (CUSE): A novel and fast technique for shear elasticity imaging. In Proceedings of the IEEE International Ultrasonics Symposium, Dresden, Germany, 7–10 October 2012; pp. 1842–1845.
60. Song, P.; Urban, M.W.; Manduca, A.; Zhao, H.; Greenleaf, J.F.; Chen, S. Comb-Push Ultrasound Shear Elastography (CUSE) with Various Ultrasound Push Beams. *IEEE Trans. Med. Imaging* **2013**, *32*, 1435–1447. [[CrossRef](#)] [[PubMed](#)]
61. Song, P.; Zhao, H.; Manduca, A.; Urban, M.W.; Greenleaf, J.F.; Chen, S. Comb-Push Ultrasound Shear Elastography (CUSE): A Novel Method for Two-Dimensional Shear Elasticity Imaging of Soft Tissues. *IEEE Trans. Med. Imaging* **2012**, *31*, 1821–1832. [[CrossRef](#)]
62. Khowailed, I.A.; Lee, Y.; Lee, H. Assessing the differences in muscle stiffness measured with shear wave elastography and myotonometer during the menstrual cycle in young women. *Clin. Physiol. Funct. Imaging* **2022**, *42*, 320–326. [[CrossRef](#)] [[PubMed](#)]
63. Maksuti, E.; Widman, E.; Larsson, D.; Urban, M.W.; Larsson, M.; Bjällmark, A. Arterial Stiffness Estimation by Shear Wave Elastography: Validation in Phantoms with Mechanical Testing. *Ultrasound Med. Biol.* **2016**, *42*, 308–321. [[CrossRef](#)]
64. Marlevi, D.; Maksuti, E.; Urban, M.W.; Winter, R.; Larsson, M. Plaque characterization using shear wave elastography—Evaluation of differentiability and accuracy using a combined ex vivo and in vitro setup. *Phys. Med. Biol.* **2018**, *63*, 235008. [[CrossRef](#)]
65. Garra, B.S. Elastography: History, principles, and technique comparison. *Abdom. Imaging* **2015**, *40*, 680–697. [[CrossRef](#)]
66. Lee, Y.; Kim, M.; Lee, H. The Measurement of Stiffness for Major Muscles with Shear Wave Elastography and Myoton: A Quantitative Analysis Study. *Diagnostics* **2021**, *11*, 524. [[PubMed](#)]

67. Okafor, L.; Varacallo, M. Anatomy, Shoulder and Upper Limb, Hand Flexor Digitorum Superficialis Muscle. In *StatPearls*; StatPearls Publishing: Treasure Island, FL, USA, 2021.
68. Baumer, T.G.; Davis, L.; Dischler, J.; Siegal, D.S.; van Holsbeeck, M.; Moutzouros, V.; Bey, M.J. Shear wave elastography of the supraspinatus muscle and tendon: Repeatability and preliminary findings. *J. Biomech.* **2017**, *53*, 201–204. [[CrossRef](#)] [[PubMed](#)]
69. Dieterich, A.V.; Andrade, R.J.; Le Sant, G.; Falla, D.; Petzke, F.; Hug, F.; Nordez, A. Shear wave elastography reveals different degrees of passive and active stiffness of the neck extensor muscles. *Eur. J. Appl. Physiol.* **2017**, *117*, 171–178. [[PubMed](#)]
70. Gennisson, J.-L.; Deffieux, T.; Macé, E.; Montaldo, G.; Fink, M.; Tanter, M. Viscoelastic and Anisotropic Mechanical Properties of in vivo Muscle Tissue Assessed by Supersonic Shear Imaging. *Ultrasound Med. Biol.* **2010**, *36*, 789–801. [[CrossRef](#)]
71. Kuo, P.-H.; Deshpande, A.D. Muscle-tendon units provide limited contributions to the passive stiffness of the index finger metacarpophalangeal joint. *J. Biomech.* **2012**, *45*, 2531–2538. [[CrossRef](#)]
72. Roberts, T.J. Contribution of elastic tissues to the mechanics and energetics of muscle function during movement. *J. Exp. Biol.* **2016**, *219*, 266–275. [[CrossRef](#)]
73. Bouillard, K.; Nordez, A.; Hug, F. Estimation of individual muscle force using elastography. *PLoS ONE* **2021**, *6*, e29261. [[CrossRef](#)]
74. Hug, F.; Tucker, K.; Gennisson, J.L.; Tanter, M.; Nordez, A. Elastography for muscle biomechanics: Toward the estimation of individual muscle force. *Exerc. Sport Sci. Rev.* **2015**, *43*, 125–133. [[CrossRef](#)]

Disclaimer/Publisher’s Note: The statements, opinions and data contained in all publications are solely those of the individual author(s) and contributor(s) and not of MDPI and/or the editor(s). MDPI and/or the editor(s) disclaim responsibility for any injury to people or property resulting from any ideas, methods, instructions or products referred to in the content.